4-2015

GEANT4 Simulation of Detector Properties in the MOLLER Experiment

Christopher R. Haufe
College of William and Mary

GEANT4 Simulation of Detector Properties in the MOLLER Experiment

A thesis submitted in partial fulfillment of the requirement
for the degree of Bachelor of Science in Physics from
The College of William and Mary

by

Christopher Randolph Skelton Haufe

Accepted for HONORS
(Honors or no-Honors)

Wouter Deconinck, Physics, Advisor

Gina L. Hoatson

Gina Hoatson, Physics

Mark Hinders, Applied Science

Williamsburg, VA
April 28, 2015

GEANT4 Simulation of Detector Properties in the MOLLER Experiment

Christopher Haufe

May 11, 2015

Abstract

To explore the existence of new physics beyond the scope of the electroweak theory, international collaborations of nuclear physicists have constructed several precision-measurement experiments. One of these is the MOLLER experiment—a low-energy parity violation experiment that will utilize the 12 GeV upgrade of Jefferson Lab's CEBAF accelerator. The motivation of this experiment is to measure the parity violating asymmetry of Møller scattering in a liquid hydrogen target. This measurement would allow for a more precise determination of the electron's weak charge and the weak mixing angle. While still in its planning stages, the MOLLER experiment requires a detailed simulation framework in order to determine how the project should be run in the future. The simulation framework for MOLLER, called "remoll", is written in C++ and uses the GEANT4 framework and libraries. It has recently been updated to include the full detector geometry of the experiment. The viability of the detector geometry in the real experiment will rely on a detailed analysis of the detector's properties through simulation. The first part of this analysis assesses the impact of particle crosstalk in the design.

Contents

1 Introduction

The MOLLER (**M**easurement **O**f a **L**epton **L**epton **E**lectroweak **R**eaction) Experiment will analyze weakly interacting electrons in order to precisely measure the weak charge of the electron (Q^e_{weak}) and the weak mixing angle (θ_W) [5]. In order to understand the full extent of the theory behind the weak interaction in Møller scattering, this document includes a brief introduction to parity violation. As a consequence, the methodological explanation of the MOLLER experiment that follows will be easier to grasp and understand. Finally, the MOLLER experiment apparatus and detector geometry will be presented and discussed.

1.1 Parity Violation

Møller scattering is the formal name given to electron-electron scattering, named after Danish physicist Christian Møller. When two electrons collide, they can interact with each other electromagnetically or weakly.

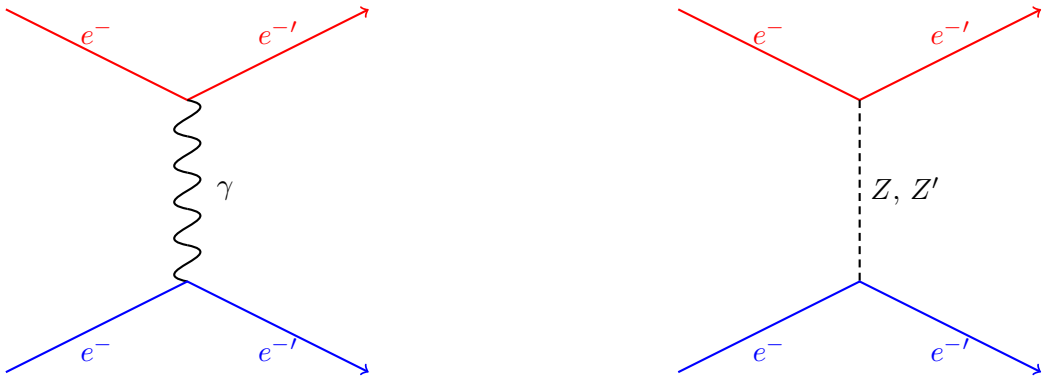

Figure 1: The Feynman diagram on the left depicts the electromagnetic interaction in Møller scattering. A photon is exchanged between the two electrons. The Feynman diagram on the right depicts the weak interaction in Møller scattering. A Z boson is exchanged between the two electrons.

The left Feynman diagram of Figure 1 depicts the electromagnetic interaction of two colliding electrons. A photon is exchanged between the electrons during the collision. Alternatively, the right Feynman diagram of Figure 1 depicts the weak interaction of the two colliding electrons. A Z boson is exchanged between the two electrons as they collide. Due to the fact that a Z boson is much heavier than a photon—a massless particle—more "virtual energy" is required for the weak interaction to occur. Therefore, the electromagnetic interaction occurs considerably more frequently than the weak interaction in Møller scattering. The MOLLER experiment is primarily concerned with the weak interaction, the only fundamental force to exhibit the phenomenon of "parity violation".

Figure 2: A graphic illustrating the difference between the right-handed and left-handed parity states. S is the direction of spin and p is the direction of momentum. Photo Credit: [7]

Parity can be best described as being analogous to a mirror. A longitudinally-polarized electron can exist in the form of two parity states: A "right-handed" parity state and a "left-handed" parity state. An electron in a right-handed parity state has a direction of spin that matches the direction of motion. An electron in a left-handed parity state has a direction of spin that is opposite the direction of motion (See Figure 2). Therefore, one parity state is a mirror image of the electron in the other parity state. In the electromagnetic interaction, the electrons of both parity states will behave the same when they scatter. This means

that the electromagnetic interaction is "parity independent"—parity is conserved in this interaction.

In early nuclear physics, it was believed that parity was conserved in all interactions. However, this notion had not been proven for the weak interaction. In 1957, physicists T.D. Lee, C.N. Yang, C.S. Wu, and others discovered that parity was not conserved in the weak interaction. In fact, it was found that only "left-helicity" fermions interacted weakly. This breakthrough was eye opening, as it was the first discovery that disproved the long cherished "law of conservation of parity"[1].

Electrons of one parity state are more likely to interact weakly than electrons of the other parity state. Therefore, we can determine how often electrons interact weakly in a Møller scattering experiment by controlling the parity of the electrons sent into each collision. Using photomultiplier tubes that convert the detection of scattered electrons into signals, we can analyze these signals for signs of parity violation.

We can also measure the interference between the electromagnetic amplitude and the weak neutral current amplitude of scattered electrons [3]. This value, called the "Parity Violating Asymmetry" (A_{pv}), tells us how often Møller electrons in the experiment interact weakly versus electromagnetically. Many collaborations that perform parity violation experiments measure A_{pv} to make precise measurements of essential electroweak constants.

1.2 The MOLLER Experiment

The MOLLER Experiment is a future parity violation experiment that will take advantage of Jefferson Lab's new 12 GeV accelerator beam upgrade. At an operational energy of around 11 GeV, the MOLLER Experiment will serve as a low-energy indirect probe that hopes to validate new physics that lies beyond the electroweak theory and the standard model.

Although the details of the experiment are still in planning stages, the basic premises are as follows. A beam of polarized electrons is injected into the CEBAF particle accelerator and travels its circumference five times until it reaches Hall A. The polarized electrons will then scatter off of unpolarized electrons in a liquid hydrogen target. The scattered electrons travel through a collimator until they reach the detector apparatus made of quartz Cerenkov detectors, aluminium light-guides, and photomultiplier tubes (more about this in section 1.3).

The electrons and secondary particles first pass through the quartz Cerenkov detectors. The index of refraction (n) of quartz is $n = 1.46$, and so the speed of light is reduced within the detector. This allows scattered electrons to travel through the detector faster than light travels through the detector. As a result, Cerenkov photons are produced.

These photons leave the Cerenkov detector, travel through the aluminium light-guide, and finally strike the photocathode of a photomultiplier tube (PMT) at the end of the light-guide. Electrons are struck off the photocathode and trigger a cascade of electrons that end up leaving the PMT as an analog signal. This signal is converted to a digital signal that is stored for future data analysis.

By comparing the composition of each signal to the parity of the electron beam at any given point in time, the experiment will measure A_{pv} to a projected overall fractional accuracy of 2.3% [2]. This value will be used to make a precise measurement of the electron's weak charge in accordance with the following equation from electroweak theory:

$$A_{pv} = mE\frac{G_F}{\sqrt{2}\pi\alpha}\frac{2y(1-y)}{1+y^4+(1-y)^4}Q^e_{weak} \tag{1}$$

In this equation, m is the electron mass, E is the incident beam energy, G_F is the Fermi constant, α is the fine structure constant, and $y \equiv 1 - E'/E$, where E' is the energy of one of the scattered electrons [5].

The electron's weak charge will be used to determine the weak mixing angle by way of the following equation, originating again from electroweak theory:

$$Q^e_{weak} = 1 - 4\sin^2\theta_W \tag{2}$$

A measurement of this kind will allow a factor of five improvement in fractional precision over the only other measurement of Møller scattering A_{pv}, done by the E158 experiment at SLAC in the early 2000's [2].

1.3 Experimental Layout

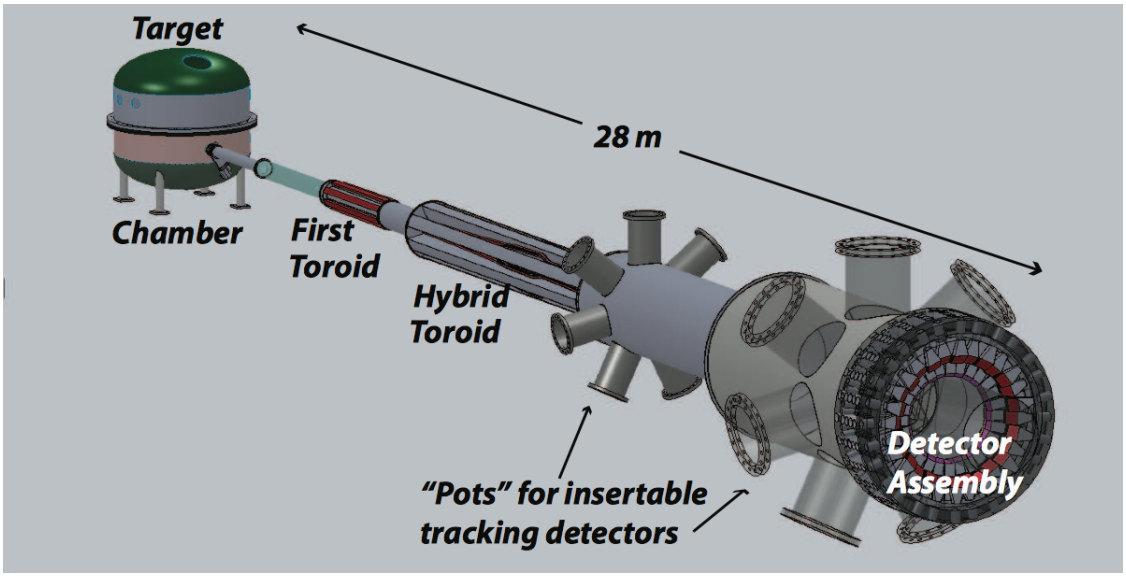

Figure 3: An overview of the experimental apparatus. Photo Credit: [3]

The current layout of the MOLLER Experiment in "remoll" is as follows. At a z-position of 0.0 is the liquid hydrogen target that contains a large number of unpolarized electrons. This is where Møller scattering takes place. The scattered electrons then travel through the main collimator, which splits the electrons into seven sections divided by

azimuthal angle (ϕ). These sections are appropriately called "septants" (see Figure 4). Since the two electrons scatter at a 180 degree angle, one electron will pass through an open septant of the collimator, where as the other electron will be blocked by the collimator. This ensures that only one of the initial scattered electrons makes it to the MOLLER detector assembly.

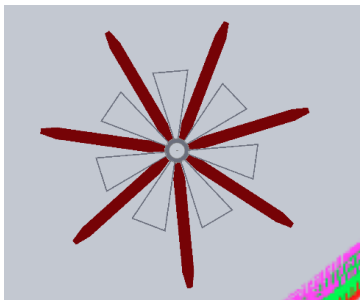

Figure 4: The front end of the main collimator. The main collimator divides the scattered electrons azimuthally into seven "septants" Photo Credit: [4]

The scattered electron and any secondary particles then travel through two toroidal magnetic fields with a series of smaller collimators between them. Finally, the particles reach the detector apparatus.

The detector apparatus is made of seven rings, each at a specific position along the beamline (z-axis). Rings 1, 2, 3, 4, and 6 contain two sub-rings of 14 Cerenkov detectors each that are staggered along the beamline. Due to the large volume of detected electrons expected at the z-positions of rings 5 and 7, both rings contain two sub-rings of 42 Cerenkov detectors each. As described in the previous section, each Cerenkov detector is connected to an aluminium light-guide that is filled with air. This connection is angled at 90 degrees (not shown in Figure 5) relative to the beam line to allow for internal reflection within the light-guide (see Figure 5) [6].

The lengths of each light-guide vary from ring to ring, such that all photomultiplier

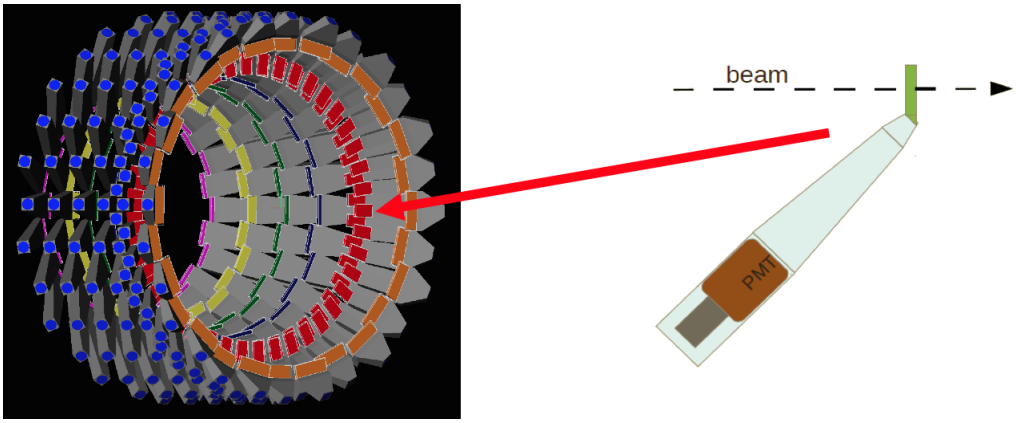

Figure 5: The graphic on the left shows the design of the detector apparatus, assembled in a ring-like structure. In the graphic, the orange, red, dark blue, green, yellow, and pink areas represent the quartz detectors (one color per ring), the grey areas symbolize the light-guides, and the blue circles represent the photocathodes of the photomultiplier tubes. The graphic on the right shows the layout of every quartz detector/light-guide/PMT combination. Although The Aluminum light-guide (clear) connects to the Cerenkov quartz block (green) at a 45 degree angle in this graphic, the simulation geometry has been changed to simulate a 90 degree angle. The PMT connects directly to the light-guide. Photo Credit: [6]

tubes in the detector apparatus are at the same radial distance from the beamline. The opening of each photomultiplier tube connects directly to the light-guide, allowing Cerenkov photons to strike the photocathode with minimal loss.

2 Methodology

In order to know with certainty that the collected data originates from Cerenkov photon generation in the quartz detector, it is important to identify instances of detector interference, or "crosstalk", in the simulation. Crosstalk refers to photon detections in the photocathode that are not generated by Cerenkov radiation in the quartz detector.

Crosstalk can exist in many forms. One form is an event where a scattered electron

travels through a quartz detector in one ring and then impacts the aluminium light-guide in the next ring. When the scattered electron collides with the aluminium atoms in the light-guide, it can produce photons and electrons that travel through the light-guide to the PMT. Additionally, if a scattered electron travels through air quickly enough, it will generate Cerenkov photons without ever impacting a quartz detector. These air-generated Cerenkov photons can easily strike any photocathode by way of the aluminium light-guide (see Figure 6).

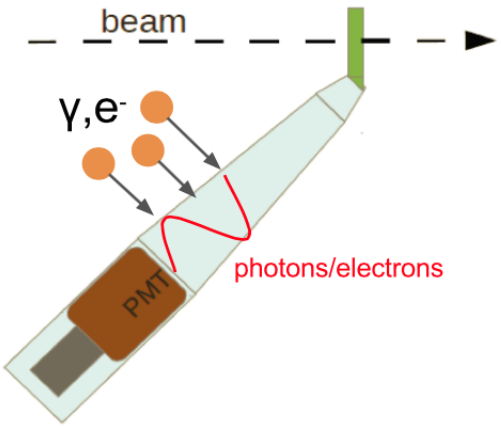

Figure 6: This graphic shows the layout of every quartz detector/light-guide/PMT combination from Figure 5. If an electron strikes an Aluminum atom in the light-guide, or if an electron generates Cerenkov radiation in air, photons and electrons can enter the light-guide directly and strike the photocathode. Both scenarios are forms of "crosstalk". (Again, the light-guide is actually positioned 90 degrees relative to the beamline instead of 45 degrees). Photo Credit: [6]

To detect instances of crosstalk within the MOLLER simulation framework, I wrote a script in C++ that directs the data analysis software package ROOT to plot hits detected by the photocathode only if these hits are suspected of being crosstalk hits (see Appendix).

The script operates as follows. First, it locates a ROOT file that contains data from

a typical GEANT4 simulation of the MOLLER experiment that includes the full detector geometry. These files typically contain about a million "events", in which one "event" is a scattering of a polarized electron off an unpolarized electron in the liquid hydrogen target. The script loads the ROOT file into memory and loops through every event. While focused on one event, the script loops through the event's "hits" (or particle detections) and checks whether or not the hit is an electron that is detected in a quartz detector. If a hit of this type is found, the identification number of that detector is stored.

The script will then loop through all photomultiplier tubes by their identification number. The identification number of a photomultiplier tube is identical to the identification number of the PMT's corresponding quartz detector. Therefore, if it is found that the identification number of the PMT matches a stored identification number of a quartz detector, all hits in this PMT are skipped. If the identification number of the PMT does not match a stored number, then photon hits in the photocathode of this PMT are plotted in a two-dimensional histogram. By the end of the event loop, all photon hits in the photocathodes that do not originate from a quartz block detection—hits that could be classified as crosstalk—are plotted for a single event.

The script continues the process described above for every event. Finally, a two-dimensional histogram is printed in ROOT that depicts the number of crosstalk hits and their locations within the photocathodes of the detector apparatus.

3 Results

3.1 Photons Outside the Optical Range

I applied the C++ script discussed in the previous section to a ROOT file containing "remoll" data from 1,000,000 events. The results of this first trial are shown in Figure 7.

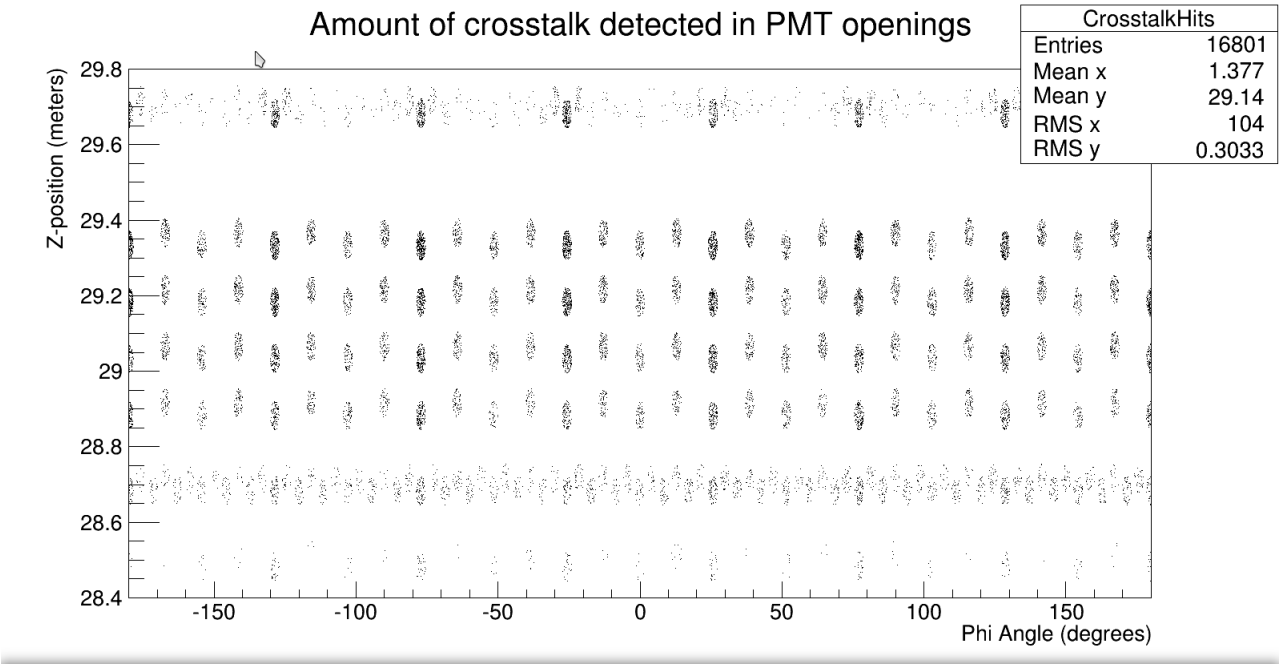

Figure 7: Plot showing the location of every non-optical photon hit from crosstalk in the photocathodes of the detector apparatus. The vertical axis shows the z-position of each detection and the horizontal axis shows the azimuthal angle (in degrees and relative to the horizontal axis perpendicular to the beam) of each detection. This data is extrapolated from a one million event simulation.

I compared these results with the plot of raw data from the same ROOT file, shown in Figure 8. All hits shown in these figures are non-optical photons, meaning that these photons are not in the visible-light range of the electromagnetic spectrum.

There were 16,801 crosstalk hits detected in the photocathodes. This is out of the

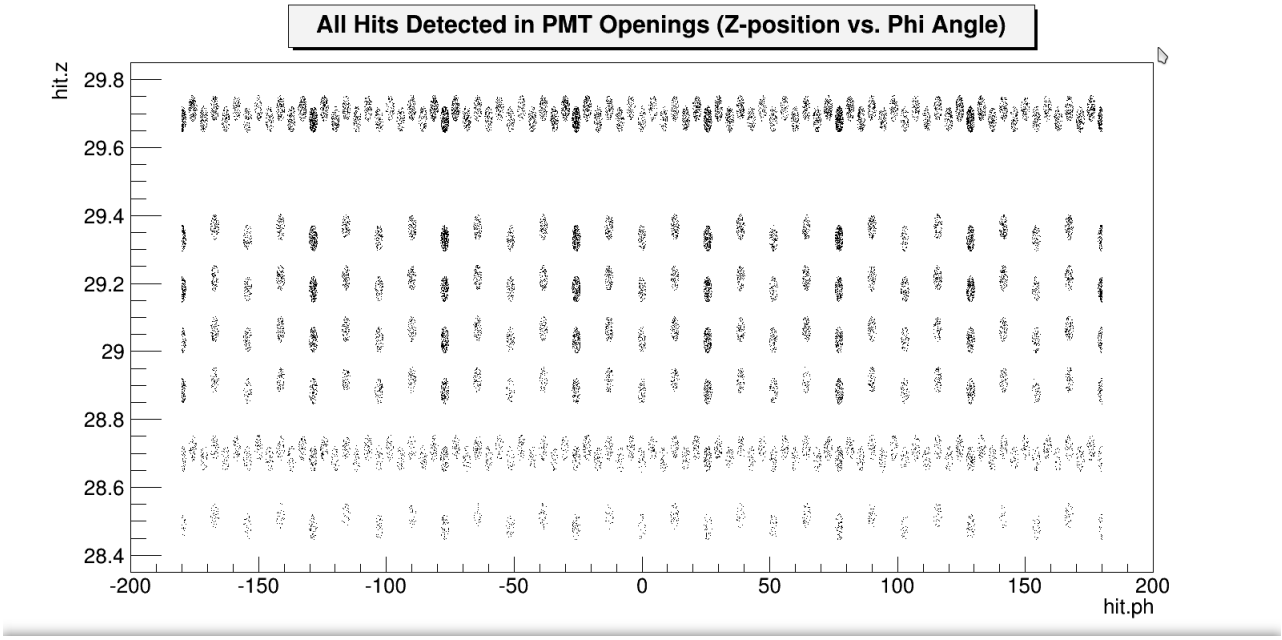

Figure 8: Plot showing the location of every non-optical photon hit in the photocathodes of the detector apparatus. The vertical axis shows the z-position of each detection (in meters) and the horizontal axis shows the azimuthal angle (in degrees and relative to the horizontal axis perpendicular to the beam) of each detection. This data is extrapolated from a one million event simulation.

total number of hits (crosstalk and non-crosstalk) detected in the photocathodes: 27,627 hits. According to the initial data, 60.8% of the non-optical photon hits detected in the photocathodes are crosstalk.

This fraction of crosstalk hits is unusually high, indicating a possible error in the code that constructs the detector geometry in the simulation.

Another consideration was that many of the crosstalk hits were generated from secondary particles, and thus a large percent of the crosstalk detected might have been background radiation. To test this hypothesis, I modified my script to plot crosstalk hits that were generated by a primary electron - an electron involved in the initial Møller scattering.

The result is shown in Figure 9.

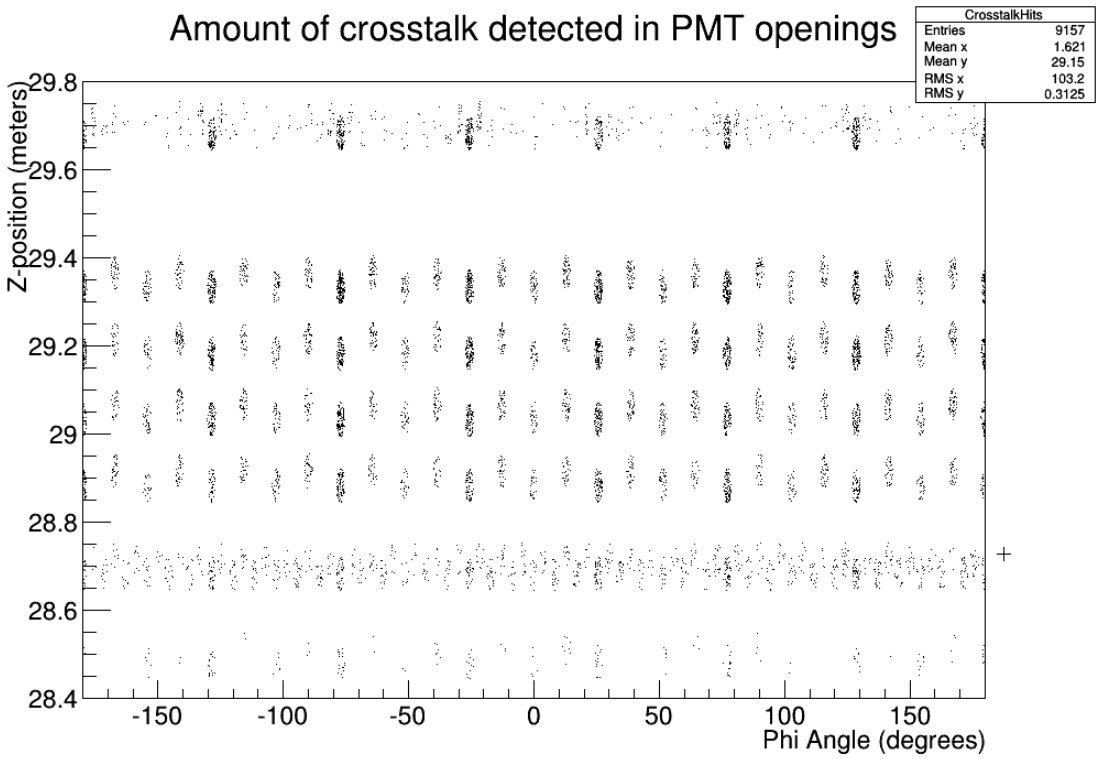

Figure 9: Plot showing the location of every non-optical photon hit from crosstalk in the photocathodes of the detector apparatus. These non-optical photons were all generated by a primary electron. The vertical axis shows the z-position of each detection and the horizontal axis shows the azimuthal angle (in degrees and relative to the horizontal axis perpendicular to the beam) of each detection. This data is extrapolated from a one million event simulation.

I compared this data to the total number of non-optical photons detected in the photocathodes. There were 9,157 non-optical photons detected in the photocathodes that were generated by primary electrons and suspected of crosstalk. This is approximately one-third of the total number of non-optical photons detected—another high value for crosstalk. This indicates that an error in the geometry code is the more likely scenario.

3.2 Photons Inside the Optical Range

Determining the magnitude of crosstalk for non-optical photons in the simulation provides useful insight on some potential problems within the design. However, determining the magnitude of crosstalk for photons in the optical range (optical photons) provides more significant insight, since most Cerenkov photons generated in the quartz detector are in the optical range.

Initially in my studies, I believed that I was plotting all photons (optical and non-optical) in the photocathodes. It was when I tried to plot only optical photons that I realized optical photons in "remoll" were not simulated correctly. In fact, optical photons were not generated in the simulation at all.

In early 2015, simulation of optical photons was implemented into "remoll" by Dr. Wouter Deconinck. Due to the large number of optical photons generated per event in the simulation, a number of structural edits were applied to the code in "remoll". Namely, various arrays in the code were changed to vectors to accommodate the large, variable sizes of optical photons per event. Additionally, most arrays in my own C++ script were changed to vectors, and cuts on non-optical photons were changed to cuts on optical photons.

The large number of optical photons generated per event would make a one million event simulation run over days instead of hours. Therefore, I restricted my analysis of optical photons to 100,000 event simulations.

I applied my edited C++ script to a new ROOT file containing "remoll" data from 100,000 events. The results of this application are shown in Figure 10. I compared these results with the plot of raw data from the new ROOT file, shown in Figure 11.

There were 169,191 crosstalk hits detected in the photocathodes. This is out of the total number of hits (crosstalk and non-crosstalk) detected in the photocathodes: 202,498 hits. According to this trial, 83.6% of optical photon hits detected in the photocathodes

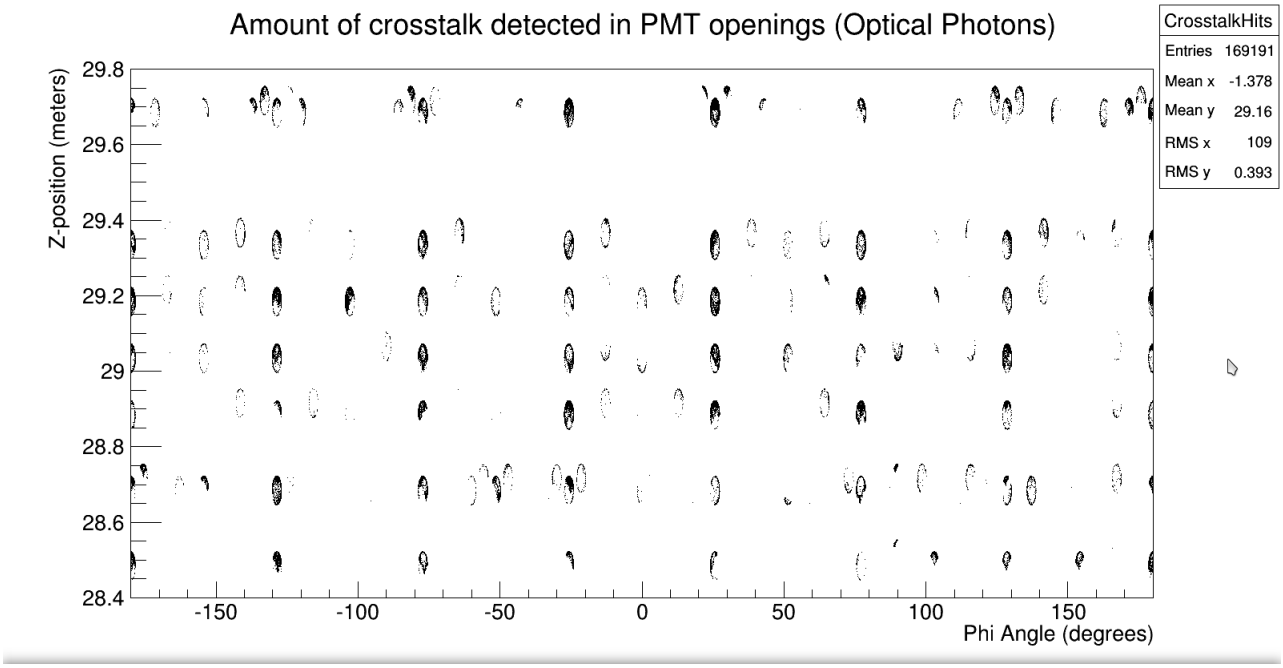

Figure 10: Plot showing the location of every optical photon hit from crosstalk in the photocathodes of the detector apparatus. The vertical axis shows the z-position of each detection and the horizontal axis shows the azimuthal angle (in degrees and relative to the horizontal axis perpendicular to the beam) of each detection. This data is extrapolated from a 100,000 event simulation.

originate from crosstalk.

Again, this fraction of crosstalk hits is unusually high, even higher than the previous trial. Following this result, I returned to the hypothesis that there was an error in the code that constructs the detector geometry in the simulation.

I ran individual simulated events using remoll's visualization software and discovered that many optical photons were either passing straight through the photocathode or through the light-guide surface. This meant that many of the non-crosstalk optical photons were missing the photocathode when they should have been detected.

I worked with graduate student Juan Carlos Cornejo to fix many of the errors in the

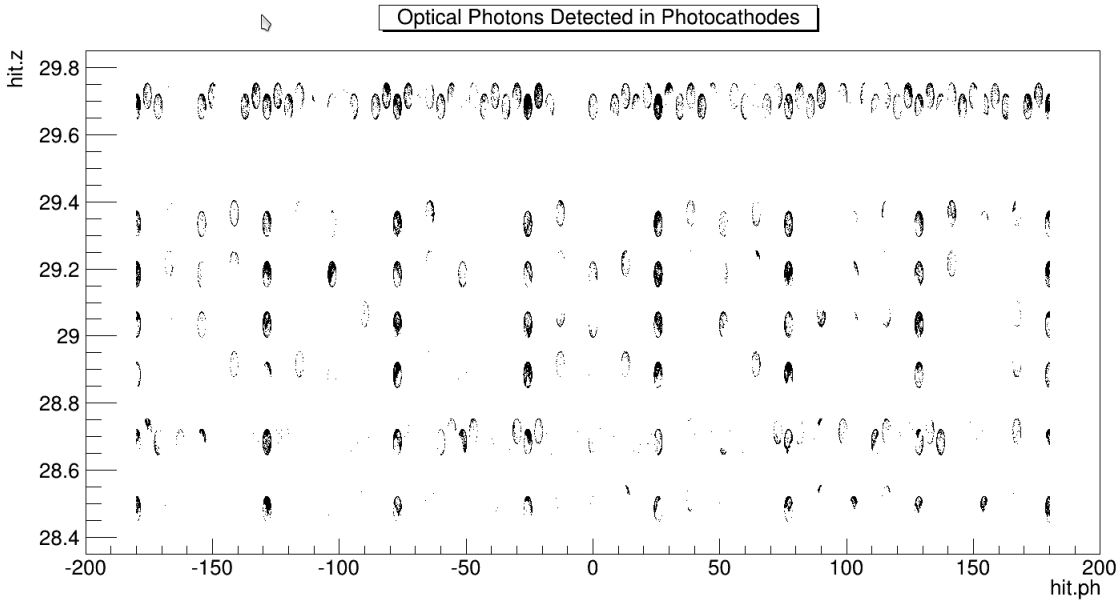

Figure 11: Plot showing the location of every optical photon hit in the photocathodes of the detector apparatus. The vertical axis shows the z-position of each detection (in meters) and the horizontal axis shows the azimuthal angle (in degrees and relative to the horizontal axis perpendicular to the beam) of each detection. This data is extrapolated from a 100,000 event simulation.

geometry. This included assigning reflectivity and transmittance values to the aluminium in the light-guide (0.91 and 0.01 respectively), adjusting the efficiency of the photocathode to 20%, and adding polished, highly reflective surfaces to the light guide and the "reflector"—the piece that connects the Cerenkov detector to the light-guide. We also discovered that the simulation was treating the PMT window as a sensitive detector instead of the photocathode. This mistake had been overlooked since the two volumes are very close to each other. We corrected this by disabling the PMT window and enabling the photocathode as a sensitive detector.

With these new adjustments, we ran the visualization software again with individual

events, and found that optical photons were reflecting normally in the light-guide (Figure 12) and were being absorbed into the photocathode (Figure 13).

In response to these improvements, I applied my C++ script to a new ROOT file containing "remoll" data from 100,000 events. The simulation in this file contained the changes that Cornejo and I made to the geometry code. The results of this final trial are shown in Figure 14. I compared these results with the plot of raw data from the new ROOT file, shown in Figure 15.

There were 987,156 crosstalk hits detected in the photocathodes. This is out of the total number of hits (crosstalk and non-crosstalk) detected in the photocathodes: 20,787,461 hits. According to this trial, 4.7% of optical photon hits detected in the photocathodes originate from crosstalk—a realistic value.

With a realistic value of the crosstalk percentage obtained, my next task was to determine where most of this crosstalk was coming from. For the simulation used in this latest trial, I disabled optical processes in the air surrounding the detector apparatus. Therefore, none of the crosstalk hits originate from Cerenkov photon generation in the air outside the detector. This was a reasonable course of action, since theoretically the amount of crosstalk from Cerenkov photon generation in the air around the detector should be negligible.

My next course of action was to determine how many of the crosstalk photons originated from primary electrons. I applied my edited C++ script to the ROOT file and obtained the results shown in Figure 16.

There were 867,238 crosstalk hits detected in the photocathodes that were generated from primary electrons, which is 87.9% of the total number of crosstalk hits and 4.2% of the total number of optical photon hits. This result indicates that a significant portion of crosstalk in the simulation originates from the two scattered electrons of each event.

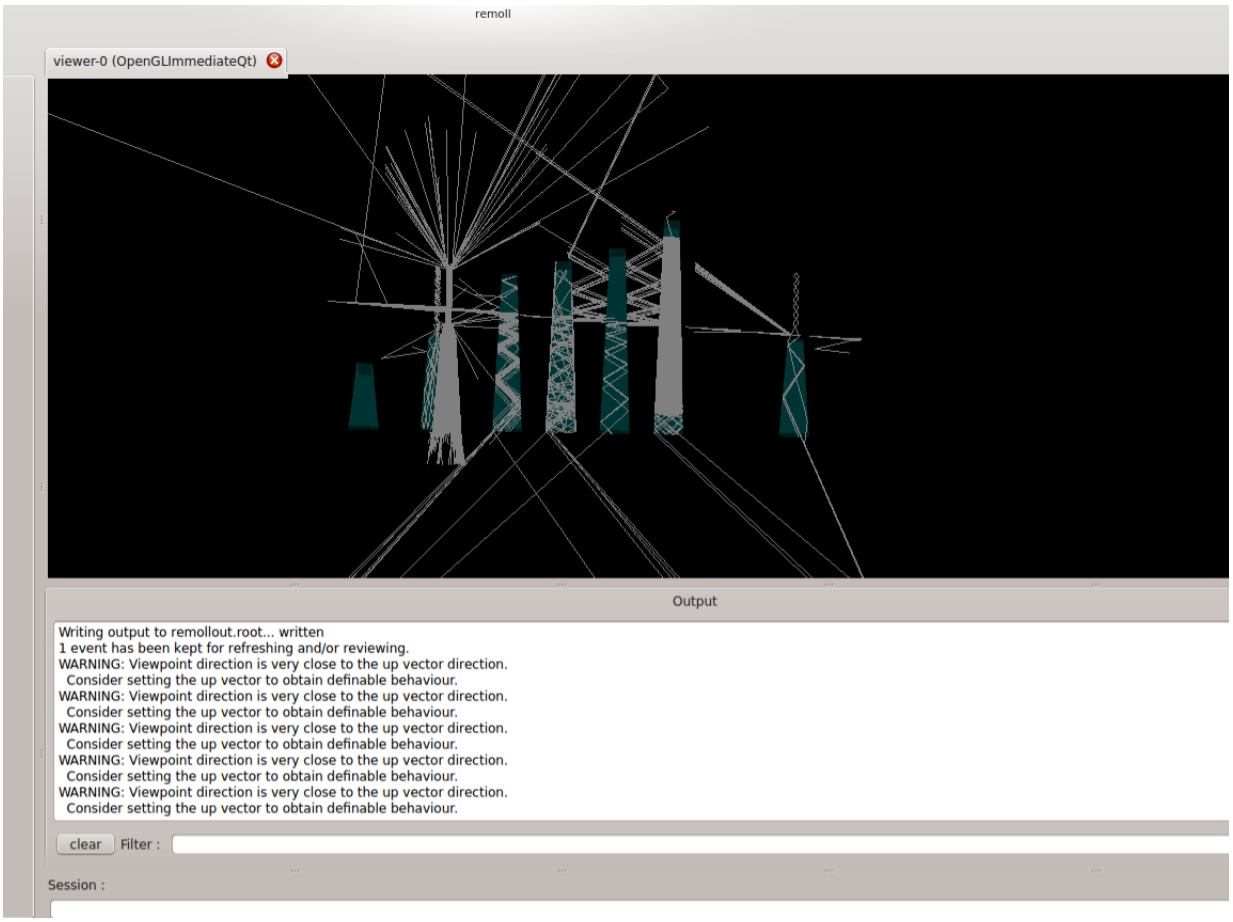

Figure 12: Visualization graphic showing the tracks of optical photons (gray) traveling through the light-guides (dark teal). These tracks enter through the quartz bars on top and reflect within the light-guide without transmitting through the light-guide's surface. The tracks that appear to exit through the bottom of the light-guide were not in the light-guide at all—they originate from the space behind these light-guides.

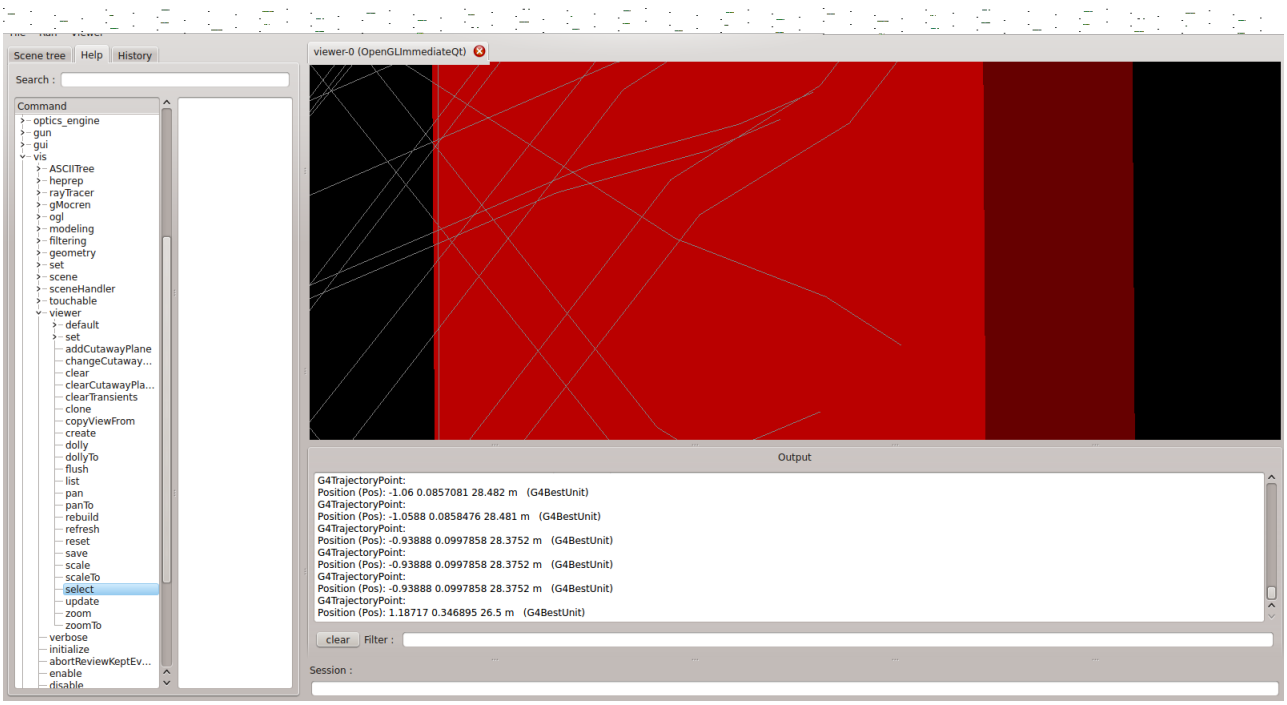

Figure 13: Visualization graphic showing the absorbance of optical photon tracks (gray) in the photocathode (red block). The efficiency of the photocathode is 20%, meaning 20% of photons striking the photocathode are absorbed, while the others are "killed" by the simulation. No optical photons are transmitted through the photocathode.

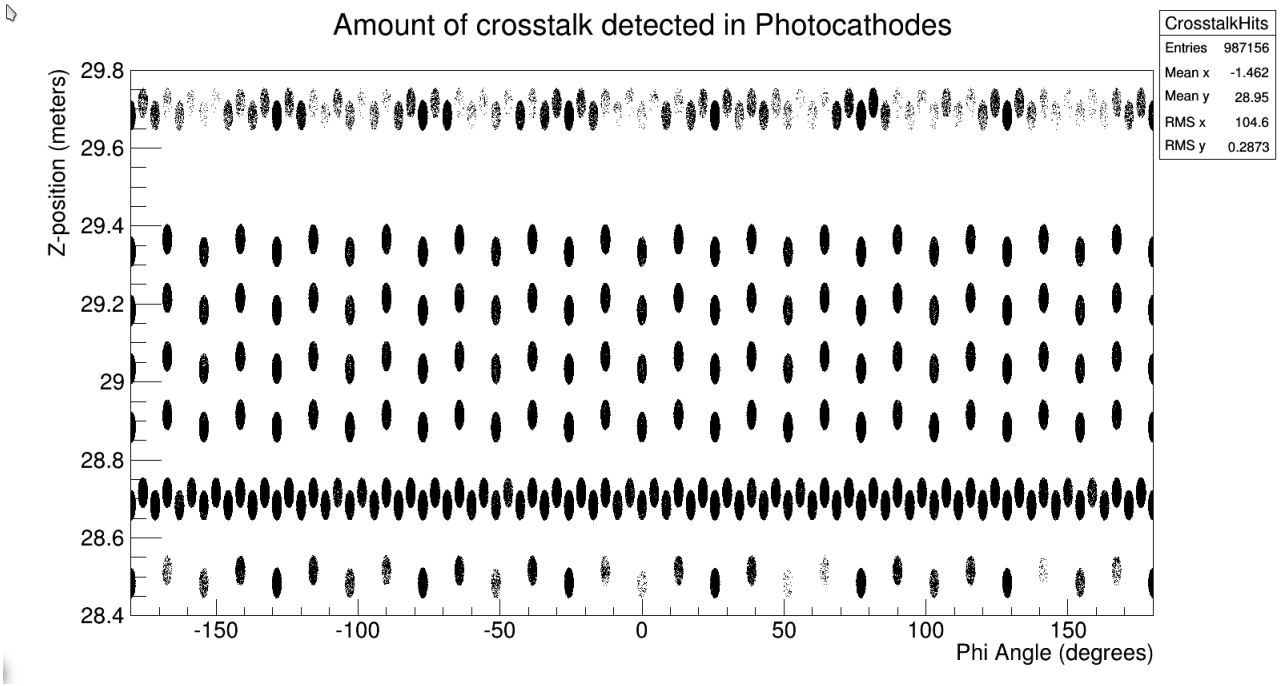

Figure 14: Plot showing the location of every optical photon hit from crosstalk in the photocathodes of the detector apparatus. The vertical axis shows the z-position of each detection and the horizontal axis shows the azimuthal angle (in degrees and relative to the horizontal axis perpendicular to the beam) of each detection. This data is extrapolated from a 100,000 event simulation.

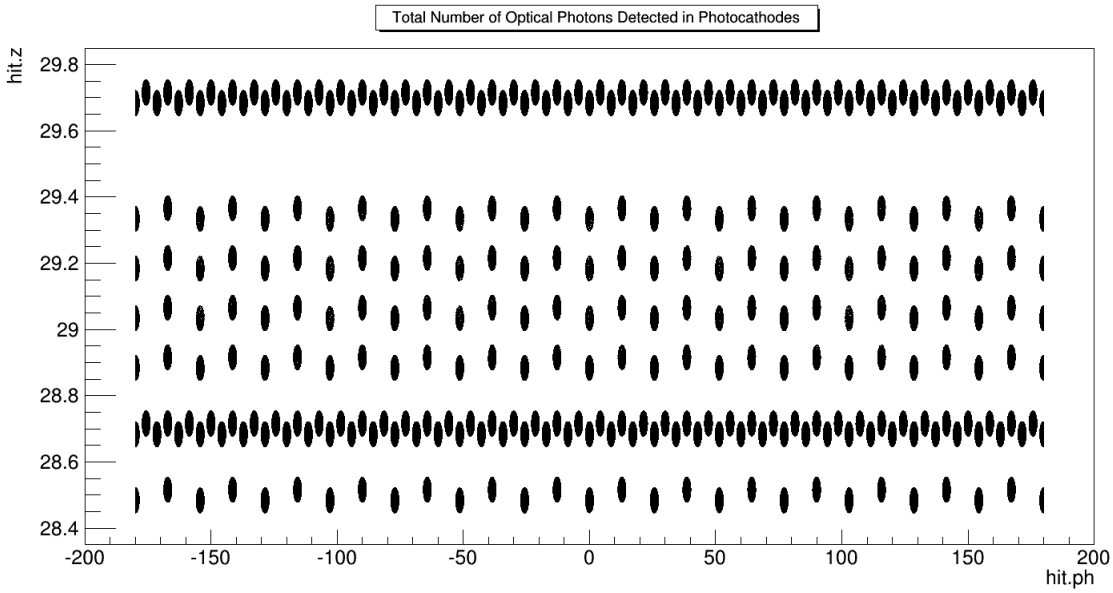

Figure 15: Plot showing the location of every optical photon hit in the photocathodes of the detector apparatus. The vertical axis shows the z-position of each detection (in meters) and the horizontal axis shows the azimuthal angle (in degrees and relative to the horizontal axis perpendicular to the beam) of each detection. This data is extrapolated from a 100,000 event simulation.

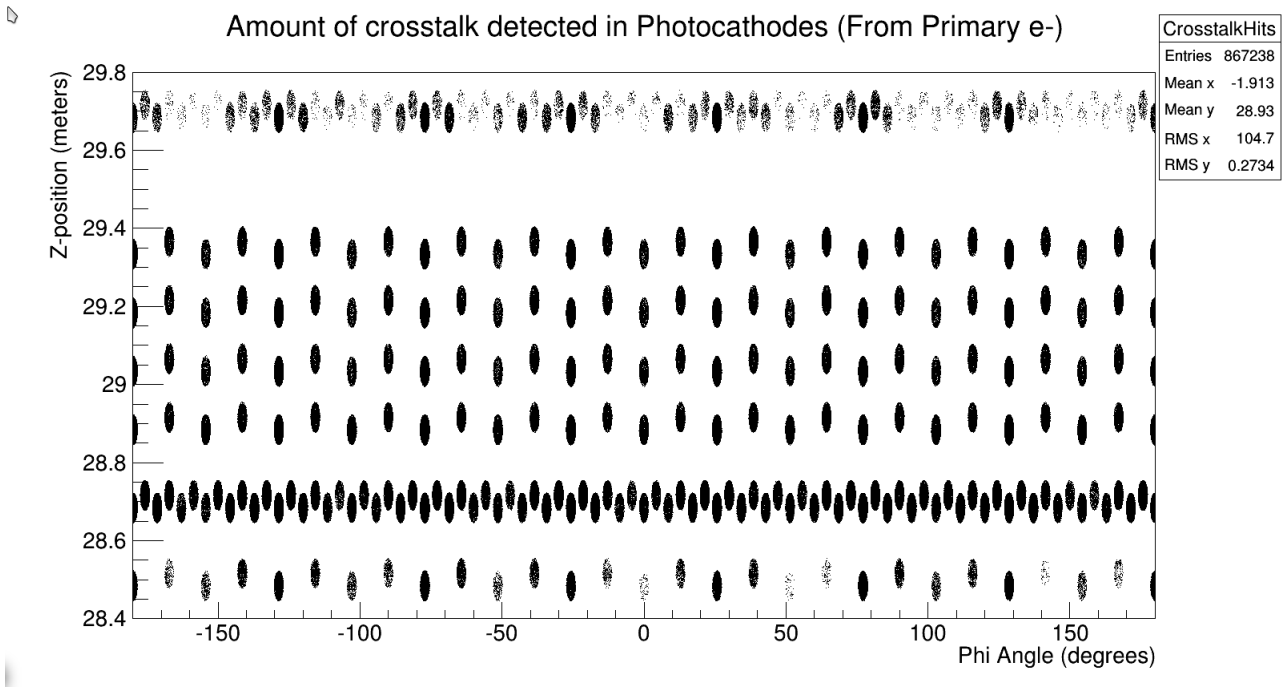

Figure 16: Plot showing the location of every optical photon hit from crosstalk in the photocathodes of the detector apparatus. These optical photons were all generated by a primary electron. The vertical axis shows the z-position of each detection and the horizontal axis shows the azimuthal angle (in degrees and relative to the horizontal axis perpendicular to the beam) of each detection. This data is extrapolated from a 100,000 event simulation.

4 Conclusion and Outlook

The initial results suggest that crosstalk plays a role in what the photocathodes detect. The magnitude of crosstalk from optical photons is substantial enough that it must be taken into account for future data analysis. The magnitude of crossstalk from non-optical photons is currently inconclusive due to the unusually large amount of crosstalk detected, but this may be resolved with the new edits to the geometry code.

In the case of optical photons, 4.7% crosstalk is a realistic value, but still a problematic value that must be taken into consideration. 87.9% of this crosstalk is generated from primary electrons, suggesting that most of the crosstalk seen in the detector assembly comes from scattered electrons passing through the light-guides. These electrons can generate Cerenkov radiation in the air of the light guide, or they can collide with the aluminium atoms in the light-guide and send particle debris into the photocathode.

The next course of action in this study is to determine which physical volumes these primary electrons pass through on an event by event basis. Do they pass through a Cerenkov detector initially before passing through a light-guide in the next ring over, or do they pass through a light-guide directly? To answer these questions, we will turn to the remoll's visualization software.

Now that an early determination of the relative crosstalk in the detector assembly has been made, we have a starting point from which we can compare other detector designs. The application of my C++ script from this study will allow MOLLER collaborators to test new detector designs and determine if less than 4.7% relative crosstalk can be achieved. Additionally, the successful implementation of optical photons in "remoll" will allow MOLLER collaborators to perform more accurate and realistic simulation studies in the future.

Appendix

```
/*******************************
Script to plot crosstalk in remoll full-detector geometry
Christopher Haufe
College of William & Mary
crhaufe@email.wm.edu
*******************************/

#include <iostream>
#include <vector>
#include "TSystem.h"
#include "TChain.h"
#include "TCanvas.h"
#include "TH2D.h"
#include "TBranch.h"
#include "TCut.h"
#include "TFile.h"
#include "TROOT.h"
#include "TLegend.h"

TH2D* CrosstalkHits;

void PlotCrosstalk()
{
  //Load library
  gSystem->Load("build/libremollroot.so");

  //Create histograms
  CrosstalkHits = new TH2D("CrosstalkHits","Amount of crosstalk
  detected in PMT openings",3600,-180,180,1000,28.4,29.8);

  //Initialize root files
  TChain* T = new TChain("T");
  T->Add("[.root file]"); \\put ROOT file directory in brackets

  //Declarations (now includes vectors to handle optical photons)
  Double_t ev_thcom;
  std::vector<Int_t> *hit_trid = 0;
  std::vector<Int_t> *hit_mtrid = 0;
```

```
std::vector<Double_t> *hit_z = 0;
std::vector<Double_t> *hit_r = 0;
std::vector<Int_t> *hit_det = 0;
std::vector<Double_t> *hit_x = 0;
std::vector<Double_t> *hit_y = 0;
std::vector<Double_t> *hit_ph = 0;
std::vector<Double_t> *hit_e = 0;
std::vector<Int_t> *hit_vid = 0;
std::vector<Int_t> *hit_pid = 0;
Double_t rate;
Int_t hit_n;

/**********************
Data Attributes:
hit.r = radial position of detection (in meters from beamline)
hit.z = z-position of detection (in meters)
hit.ph = azimuthal angle of detection (in degrees relative to
                                       axis perpendicular to beam)
hit.vid = identification number for PMT and quartz detector
hit.pid = identification number for particle
          hit.pid==0: optical photon
          hit.pid==11: electron
          hit.pid==22: non-optical photon
hit.n = number of hits in one event
**********************/

//Set Branch Addresses
T->SetBranchAddress("hit.n",&hit_n);
T->SetBranchAddress("ev.thcom",&ev_thcom);
T->SetBranchAddress("hit.trid",&hit_trid);
T->SetBranchAddress("hit.mtrid",&hit_mtrid);
T->SetBranchAddress("hit.z",&hit_z);
T->SetBranchAddress("hit.r",&hit_r);
T->SetBranchAddress("hit.det",&hit_det);
T->SetBranchAddress("hit.x",&hit_x);
T->SetBranchAddress("hit.y",&hit_y);
T->SetBranchAddress("hit.ph",&hit_ph);
T->SetBranchAddress("hit.e",&hit_e);
T->SetBranchAddress("hit.vid",&hit_vid);
T->SetBranchAddress("hit.pid",&hit_pid);
T->SetBranchAddress("rate",&rate);
```

```
//Retrieve number of events from root file
Long64_t nentries = T->GetEntries();

//Loop through all events
for (Long64_t i=0; i<nentries;i++)
{
  //Print out of script progress
  if (i%10000 == 0)
  {
     cout << "Event # " << i << endl;
  }

//Initialize vector to store quartz block hits
std::vector<Int_t> *quartz;

//Declare other parameters
Double_t hit_zdir = 0.0;
Double_t hit_phi = 0.0;
Int_t BadHit = 0;

//Retrieve the next event
T->GetEntry(i);


  //Loop through event hits to find hits in quartz blocks
  for(int a = 0; a < hit_n; a++)
  {
              if(hit_z->at(a)>28.2 && hit_r->at(a)<1.3 &&
                  hit_pid->at(a)==11)
              {
                  quartz.push_back(hit_vid->at(a));
              }
              else
              {
                  quartz.push_back(0);
              }
  }
```

```
    //Loop through PMT's to fill histogram with PMT hits...
    //...when there are no corresponding quartz block hits
    for(int pmtID = 5; pmtID < 3146; pmtID+=10)
    {
                for(int a = 0; a < hit_n; a++)
                {
                        if(quartz[a]==pmtID)
                        {
                                BadHit = 1;
                                break;
                        }
                }
                if(BadHit==1)
                {
                        continue;
                }
                for(int a = 0; a < hit_n; a++)
                {
                        if (hit_z->at(a)>28.2 && hit_r->at(a)>1.3
                            && hit_pid->at(a)==0 \\or 22
                            && hit_vid->at(a)==pmtID)
                        {
                                hit_zdir=hit_z->at(a);
                                hit_phi=hit_ph->at(a);
                                CrosstalkHits->Fill(hit_phi,hit_zdir);
                        }
                }
        }
  }


//Draw Histogram
TCanvas* c1 = new TCanvas("c1");
c1->cd();

CrosstalkHits->GetXaxis()->SetTitle("Phi Angle (degrees)");
CrosstalkHits->GetYaxis()->SetTitle("Z-position (meters)");
CrosstalkHits->SetLineColor(kBlue);
CrosstalkHits->Draw();
}
```

References

1 K. Mynemi, "Symmetry Destroyed: The Failure of Parity." History of Science: Parity Violation. December 10, 1984. Accessed December 2, 2014. http://www.hep.ucl.ac.uk/˜nk/teaching/PH4442/parity-violation.html.

2 K.S. Kumar, "The moller experiment: An ultra-precise measurement of the weak mixing angle using parity-violating moller scattering," Unpublished manuscript, Physics Department, University of Massachusetts, Amherst, Amherst, MA, 2012.

3 K.S. Kumar, "The moller experiment: An ultra-precise measurement of the weak mixing angle using parity-violating moller scattering," Unpublished manuscript, Physics Department, University of Massachusetts, Amherst, Amherst, MA, 2010.

4 K.S. Kumar, "Context for the MOLLER Experiment: Global Perspective and Experimental Technique," Unpublished presentation, Physics Department, SUNY Stony Brook University, Stony Brook, NY, 2014.

5 K.S. Kumar, "The MOLLER Experiment: An Ultra-Precise Measurement of the Weak Mixing Angle using Møller Scattering," Unpublished manuscript, Physics Department, SUNY Stony Brook University, Stony Brook, NY, 2014. (arXiv:1411.4088v2)

6 M. Gericke, "Integrating Detector Project," Unpublished presentation, Thomas Jefferson National Accelerator Facility, Newport News, VA, 2014.

Image Credits:

7 Chirality (Physics), Wikipedia: http://en.wikipedia.org/wiki/Chirality_(physics)